Research Square

Preprints are preliminary reports that have not undergone peer review.
They should not be considered conclusive, used to inform clinical practice,
or referenced by the media as validated information.

Disease Associated Loss of an MHC Locus in the Tasmanian Devil: Evolutionary Consequences for Devil Facial Tumour Disease Resistance

Carolyn Hogg

carolyn.hogg@sydney.edu.au

The University of Sydney https://orcid.org/0000-0002-6328-398X

Kimberley Batley

The University of Sydney

Ruth Pye

University of Tasmania

Luke Silver

The University of Sydney https://orcid.org/0000-0002-1718-5756

Katherine Farquharson

The University of Sydney

Yuanyuan Cheng

The University of Sydney

Andy Flies

University of Tasmania

Katherine Belov

University of Sydney

Article

Keywords:

Posted Date: July 8th, 2026

DOI: https://doi.org/10.21203/rs.3.rs-10221437/v1

License: This work is licensed under a Creative Commons Attribution 4.0 International License.
Read Full License

Additional Declarations: There is **NO** Competing Interest.

Disease-Associated Loss of an MHC Locus in the Tasmanian Devil: Evolutionary Consequences for Devil Facial Tumour Disease Resistance

Kimberley C. Batley[1†], Ruth J. Pye[2†], Luke W. Silver[1,3], Katherine A. Farquharson[1,3], Yuanyuan Cheng[1] Andrew S. Flies[2†,] Carolyn J. Hogg[1,3†*], Katherine Belov[1,3†]

[1] School of Life and Environmental Sciences, The University of Sydney, Sydney, NSW, 2006, Australia.
[2] Menzies Institute for Medical Research, University of Tasmania, Hobart, TAS, 7000, Australia.
[3] ARC Centre of Excellence for Innovations in Peptide and Protein Science, The University of Sydney, Sydney, NSW, 2006, Australia.

* Corresponding author: Professor Carolyn Hogg
Email: carolyn.hogg@sydney.edu.au
[†]equal contribution

Abstract

Transmissible cancers in the Tasmanian devil (*Sarcophilus harrisii*) provide a rare natural experiment for understanding how strong, contemporary disease pressure shapes vertebrate immune gene evolution. The emergence and spread of devil facial tumour disease (DFTD) have long been hypothesised to favour host–tumour MHC dissimilarity and to drive selection at MHC class I (MHC-I) loci, yet direct empirical evidence has been lacking. Here we demonstrate, for the first time, disease-mediated loss ("death") of an MHC-I locus in the wild. These findings extend the classical birth-and-death model by showing that "death" of an MHC locus can be an adaptive, disease-driven process, rather than only a passive outcome of duplication and relaxed constraint. Using long-read MHC genotyping combined with temporal population sampling and a functional immune phenotype, we show that devils whose MHC-I alleles differ from those expressed by devil facial tumour 1 (DFT1) cells are more likely to mount alloreactive antibody responses. A non-functional deletion of the classical MHC-I gene *Saha-UA* is strongly associated with antibody production, and this deletion has increased in frequency across multiple DFTD-affected sites within just a few generations. In parallel, MHC-I supertypes shared with the tumour (notably supertype 2) have declined in frequency, demonstrating directional selection against tumour-matching alleles and reshaping of MHC-I gene architecture at the population level. In contrast, MHC-I allele frequencies remained stable at the only long-term DFTD-free site, confirming that these shifts are disease-driven rather than neutral drift. These findings provide the first clear evidence of pathogen-driven contraction of MHC-I diversity in a wildlife species. While this evolutionary response may enhance resistance to DFT1, the loss of MHC-I diversity may reduce future resilience to emerging pathogens, underscoring the importance of maintaining immunogenetic variation in ongoing conservation management.

Background

Major histocompatibility complex class I (MHC-I) genes are among the most polymorphic regions of the vertebrate genome and play a central role in immune surveillance (Barker et al., 2023; Trowsdale & Parham, 2004). Classical MHC-I molecules are expressed on most nucleated cells and present intracellular peptides to $CD8^+$ cytotoxic T cells, enabling recognition of infected or abnormal cells (Bjorkman & Parham, 1990; Cresswell et al., 2005). The extraordinary diversity of MHC-I reflects its importance in distinguishing self from non-self and facilitating effective immune responses against a wide range of pathogens (Hughes & Nei, 1992; Radwan et al., 2020; Sommer, 2005). Over evolutionary time, MHC genes are thought to evolve under a birth-and-death model, in which gene duplication generates new loci while others are lost through deletion or pseudogenisation, producing lineage-specific immune repertoires (Hughes & Nei, 1992; Nei et al., 1997). Comparative genomic studies provide strong support for this framework, including lineage-specific loss of MHC class II loci and variation in MHC-I copy number across taxa (Minias et al., 2019; Silver et al., 2024). However, most evidence for MHC gene "death" comes from macroevolutionary comparisons, where loss is generally interpreted as the longer-term consequence of duplication, functional redundancy, relaxed purifying selection and eventual pseudogenisation. Whether contemporary disease pressure can instead directly favour the loss of a functional MHC gene within natural populations remains unresolved. In wild populations, pathogen-mediated selection is usually detected as shifts in allele or supertype frequencies within existing loci (Müller-Klein et al., 2025). For example, in East Asian frogs with long-term exposure to chytrid fungus (*Batrachochytrium dendrobatidis*, Bd), conservation of MHC-IIb supertypes ST-1 and ST-2 suggests selection for Bd resistance (Lau et al., 2023). By contrast, it has proven exceptionally difficult to show that a specific infectious agent has driven the "death" of a functional MHC gene. Real-time examples of disease-driven MHC gene loss in vertebrates are therefore, to our knowledge, lacking.

A unique opportunity to study MHC evolution within species comes from investigating transmissible cancers. Transmissible cancers are extremely rare in nature, with only three transmissible cancers reported in two species of mammals (Murgia et al., 2006; Pearse & Swift, 2006; Pye et al., 2016b). Transmissible cancers are a rare type of cancer that spreads between individuals through physical contact, and the successful engraftment and proliferation of tumour cells in a new host requires modulation or evasion of the new host animal's immune system. Central to this is the MHC, which typically shows extremely high levels of polymorphism and is able to present a great diversity of peptides that should allow the tumour cells to be identified as foreign by the host immune system. Low MHC-I diversity within species increases the probability of matched MHC-I alleles in tumours and hosts, thus reducing or eliminating the allograft response (Belov, 2011). In cases where the host and tumour MHC-I are not matched, the tumour cells must evade the allograft response, which can be accomplished by downregulation of MHC-I on the surface of tumour cells.

Genomic research suggests that the canine transmissible venereal tumour (CTVT), a sexually transmitted cancer in dogs, originated in an ancestral canid and has persisted for thousands of years

as a clonally transmissible cancer (Murchison et al., 2014). Its early spread may have been facilitated by low immunogenetic diversity in the host population (Belov, 2011), with only 148 MHC-I alleles detected in dogs and Gray wolves to date (Maccari et al., 2025), compared to more than 20,000 alleles in humans (Barker et al., 2023). Additionally, dogs have only one MHC-I gene, compared to three genes in humans. Tasmanian devils (*Sarcophilus harrisii*) also have three MHC-I genes, but like dogs have a relatively low number of MHC-I alleles and are affected by transmissible cancers (Belov, 2012).

Devils have undergone rapid and widespread population declines following the recent emergence of devil facial tumour disease (DFTD) (Cunningham et al., 2021; Lachish et al., 2007; Lazenby et al., 2018). DFTD is caused by two genetically distinct clonal transmissible cancers, DFT1 (Loh et al., 2006a; Loh et al., 2006b) and DFT2 (Pye et al., 2016b), that are passed between individuals through biting during social interactions (Hamede et al., 2013). DFT1 was first observed in 1996 and is predicted to have emerged in 1986 and has since spread across most of Tasmania, while DFT2 was identified in 2014 and is predicted to have emerged in 2011 and remains restricted to southeast Tasmania (Stammnitz et al., 2023). Both DFT1 and DFT2 are evolving under selective pressures imposed by host immunity and population structuring (Kwon et al., 2020; Stammnitz et al., 2023). A central axis of this evolutionary interaction is modulation of MHC-I expression, which directly influences tumour transmissibility, immune recognition, and disease outcome (Hussey et al., 2022; Siddle & Kaufman, 2013; Siddle et al., 2007; Siddle et al., 2013). Herein this paper is focussed on changes in Tasmanian devils as a result of the high selective pressure of DFT1 and so hereafter any mention of DFTD refers to DFT1.

DFT1 has evolved a highly effective mechanism of immune evasion through epigenetic down-regulation of MHC-I (Siddle et al., 2013). Further evidence of the importance of MHC-I comes from a small number of wild devils that have undergone spontaneous DFT1 regression and possess serum antibodies against DFT1 cells expressing surface MHC-I (Pye et al., 2016a). Additionally, anti-MHC-I antibodies have also been detected in captive devils following immunotherapy-associated DFT1 regression (Tovar et al., 2017). Experimental knockout of the MHC-I accessory gene β2-microglobulin confirms that MHC-I is the primary antibody target (Ong et al., 2021). Together, low host MHC diversity (Belov, 2011; Cheng et al., 2012a; Cheng & Belov, 2014; Cheng et al., 2012b; Morris et al., 2013) and tumour-intrinsic MHC modulation (Siddle & Kaufman, 2013, 2015) enable the cancer cells to behave as a successful allograft (Kreiss et al., 2011).

Early research into devil MHC-I identified three classical genes - Saha-UA, Saha-UB, Saha-UC - that are closely related and highly similar in sequence (>97%), likely reflecting recent gene duplications (Cheng et al., 2012a), suggesting that this gene family may remain evolutionarily dynamic. A long-read amplicon approach identified 61 MHC-I alleles with four of these shared with DFT1 cells (Cheng, *unpublished data*). Individual devils carry between one and six functional MHC-I alleles as a result of structural variation resulting in non-functional alleles (Cheng et al., 2022; Cheng et al., 2012a). The most common is a ~1.6 kb deletion that results in a Saha-UA pseudogene and is present at the highest frequency in northwest Tasmania (54.8%; (Cheng et al., 2012a)). Due to the loss of Saha-UA increasing antigenic dissimilarity between host and tumour, Cheng et al. (2012a)

hypothesised that the high Saha-UA deletion in the northwest of Tasmania would confer some type of resistance and slow the spread of DFT1 in the northwest (Fig. 1A).

Here we test the hypothesis that devils that are most genetically dissimilar to the tumour at MHC-I alleles are more likely to mount anti-MHC-I antibody responses, and that the high mortality imposed by DFT1 will favour the survival of individuals carrying fewer MHC-I alleles matched to the tumour. To test these hypotheses, we (1) determined whether host MHC-I genotypes are associated with the presence or absence of anti-MHC-I antibodies, and (2) investigated temporal changes in MHC-I allele frequencies in wild devil populations affected by DFT1. We genotyped the MHC-I (UA, UB, and UC) loci, using long-read sequencing, in two DFT1 cell lines and in 61 wild devils with DFT1 and/or serum antibody responses; and analysed MHC-I diversity in a further 531 devils from nine Tasmanian field sites born between 2012 and 2021. By linking MHC-I genotype to a functional immune phenotype in the wild and documenting parallel allele-frequency shifts across populations, we directly test whether a naturally occurring disease can drive contemporary MHC gene loss in a wild vertebrate.

Results

Wild devils with anti-DFT1 immune responses

To identify devils that mounted an immune response to DFT1, we analysed 116 serum samples from wild devils at six diseased sites (Fig. 1A; Fentonbury, Kempton, Stony Head, wukalina, Granville Harbor and Narawntapu National Park). Samples were collected from individuals aged two years and older during routine field monitoring between 2015 and 2023. Serum samples were analysed for antibodies against DFT1 cell line C5065 that does not express surface MHC-I (MHC-I- DFT1 cells), and DFT1 C5065 cells treated with interferon gamma (IFN-γ) to induce surface expression of MHC-I proteins (MHC-I+ DFT1 cells). A total of 25 individuals had anti-MHC-I antibodies, of these, 12 had clinical signs of DFT1 and 13 showed no clinical signs (Table S1). For downstream genetic analysis, these 25 individuals plus another 36 individuals with clinical signs of DFT1 but no anti-MHC-I antibodies were selected to ensure that devils had been exposed to DFT1 (N = 61) (Table S1).

Out of the13 devils with antibodies and no clinical signs of DFT1, six devils were aged 4-years or older (including two 6-year-olds and one 7-year-old). This is unusual as devils in diseased populations rarely live beyond 3-years of age (Lazenby 2018). Notably, one of the devils with anti-MHC-I antibodies and no DFT1 had undergone tumour regression (Fig. 2, Ki; Table S1 Ki), and three others remained free of DFT1 and positive for serum anti-MHC-I antibodies when they were trapped over two or more years (Fig. 2, Sy; Table S1 Sy, Ty, Ga).

Anti-DFT1 immune responses correlate with MHC-I mismatches

We performed long-read MHC-I amplicon sequencing as per Cheng et al. (2022), on the 61 devils with DFT1 and/or antibodies as well as two DFT1 cell lines (C5065 and 1426). We identified 72% (44/61) of these devils having non-functional MHC-I alleles, with the number of functional alleles per individual in this dataset ranging between three and six (Table S1). Alleles were grouped into supertypes based on the biochemical properties of variable peptide-binding residues in the encoded proteins, as per Cheng et al. (2022).

Generalized linear models (GLM) showed that age and genetic similarity (between host and DFT1) at the supertype level were strong predictors of the anti-DFT1 antibody response (ΔAICc< 2). Specifically, devils with more mismatches to DFT1 at MHC-I loci are more likely to mount an immune response, especially at the UA loci (Table S2), and survive to an older age. We then ran models at the allele and supertype level to understand whether specific alleles or supertypes are driving this pattern. A deletion at the UA locus had a strong positive effect on antibody response ($p < 0.01$; Fig. 1B), whereas the UC allele (UC*04:02:01:01) - shared with DFT1 - had a strong negative effect ($p < 0.01$; Table S3). At the supertype level, supertype 2 (also shared with DFT1) also had a strong negative response on the antibody response ($p < 0.01$; Fig. 1C; Table S3).

Of the 25 devils with anti-DFT1 antibody responses, 23 (92%) had zero matches to DFT1 at the UA loci, and through a hierarchical cluster analysis, cluster away from the two DFT1 cell lines (Fig. 3, Table S1). Additionally, eight (32%) of the 25 devils with an antibody response had at least one functional supertype not shared with DFT1 (Supertypes 1 and 7) (Fig. 3). The frequency of these supertypes was low in our dataset and were either not included in the statistical analysis, or were not strong predictors of the antibody response, likely due to small sample sizes (e.g., low frequency).

Based on transplant scoring used in human medicine to assist in selection of suitable organ donors (Kok et al., 2023; Laging et al., 2014; Tran et al., 2011), we assigned transplant scores to each of the 116 devils with serum antibody data. For each devil, each of the UA, UB and UC alleles (six in total) was given a 0 if the supertype matched that of DFT1, or a 1 for a mismatch. A devil with a complete match to DFT1 therefore had a score of 0 whereas a complete mismatch had a score of 6 (Fig. S1). There was a significant positive association between transplant score and antibody responses, with devils with higher transplant scores more likely to have serum antibodies than devils with lower scores (Fig S1A). This was also evident in our subset of 61 devils that had DFT1 and/ or serum antibodies (Fig S1B).

Predicted probabilities of UA deletion in wild populations

To expand upon our findings of correlations between MHC-I alleles and supertypes and an anti-DFT1 immune response, we next investigated, whether a) the predicted probabilities of non-functional UA (deletion) changed in devil populations over time, and whether b) the frequency of the UA deletion was higher in older age classes. We MHC genotyped an additional 531 devils (592 in total) born between 2012 and 2021 across nine field sites (Fig. 1A) and compared trends to those observed across neutral data (presented in Schraven et al., 2025). Note, four sites (Buckland, Narawntapu, Stony Head, wukalina) have been genetically managed through supplementation of healthy devils (Fig. 1A; (Fox & Seddon, 2019; McLennan et al., 2024)), however, no translocated or hybrid individuals were included in the dataset to ensure observed signals were in response to DFT1 and not supplementation.

We observed an overall increase in the predicted probability of the UA deletion (not shared with DFT1) from approximately 10 years since the arrival of DFT1 (Fig. 1B). This is in contrast to the decline in predicted probability of supertype 2 (shared with DFT1) at all field sites (Fig. 1C). These trends correlated with the frequencies of the non-functional allele and supertype 2, while no trends were

observed in the neutral data (Fig. S2). There were two long-term disease sites, wukalina and Kempton that showed decreased predicted probability of the UA deletion (Fig. 1B). DFT1 has been present for over 28 years at wukalina, and a high frequency of devils with the non-functional UA allele was observed when the first samples were collected in 2014 (Fig. S2). At Kempton, a strong decline in the predicted probability of the non-functional UA was observed (Fig. 1B), however, the predicted probability of supertype 7 (not shared with DFT1) showed a strong increasing trend (Fig. 1D).

The trend for increasing frequency of UA deletion was particularly evident at Buckland, Stony Head and Fentonbury, where DFTD has been present for ~15 years, with no observable changes in neutral diversity over the study period (Fig. S2). This trend is not observed at Granville Harbour, where disease has only been present for 9 years. In comparison to the DFT1-affected sites, the predicted probabilities of the non-functional UA deletion, supertype 2 and supertype 7 remained steady at Woolnorth, which was disease-free at the conclusion of fieldwork for this study (Fig. S4).

Comparing the frequency of the non-functional UA allele, supertypes not shared with DFTD (supertypes 1 and 7) and supertype 2 in different age classes showed that at disease sites, the frequency of the non-functional UA allele was higher in devils that lived to at least 4-years of age, compared with 1-year-olds (Table 1A & B). This is particularly evident when we calculated the frequency of the most common supertypes that are not shared with DFT1 (supertypes 1, 7 and the non-functional UA) within each age class. All animals from disease sites that were sampled at >= 5-years of age did not share a UA allele with DFT1, nor did a high proportion of 3- and 4-year-olds (Table 1C). In most cases, the contrast of this was observed for supertype 2. In keeping with the temporal trends, the frequency of both alleles at Woolnorth was similar between all age classes. Altogether these data suggest that DFT1 is driving selection for the loss of UA, increasing the chance of allorecognition of MHC-I+ DFT1 cells.

Evidence of MHC birth in devils

To investigate the "birth" of the current MHC genes in devils, we used biser (Išerić et al., 2022). The results identified segmental duplications on the scaffold NC_045429.1 at the three locations of the UA, UB and UC genes originating from another gene annotated as a MHC-I gene on the same scaffold, that we annotated as Saha-UD, suggesting that UA, UB and UC have evolved by gene duplications from UD.

We calculated the dS and divergence times between devil MHC class I genes as ranging between 0.0038 –1.1103 and 0.66 – 194.03 MYA, respectively (Table S5). Divergence times between the three classical genes ranged between 0.66 and 2.01 MYA, these estimates of divergence time are far more recent than the divergence time of devils and their closest relatives, quolls (10-15MYA) (Duchêne et al., 2018). We suggest that these three genes evolved from UD between 20.75 and 44.22 MYA.

Discussion

This study demonstrates that devil facial tumour disease (DFTD) is imposing a strong, contemporary, and directional selection on the major histocompatibility complex class I (MHC-I) repertoire of Tasmanian devils. Devils that are most genetically dissimilar to the tumour at MHC-I loci are significantly more likely to mount serum antibody responses against DFT1 cells, and these mismatched MHC-I genotypes are increasing in frequency across multiple DFTD-affected populations. Two signals dominate this pattern: loss of the classical MHC-I Saha-UA gene is strongly associated with antibody production, and the frequency of MHC-I alleles and supertypes shared with DFT1 are declining. In contrast, at the only long-term DFT1-free site in this study (Woolnorth) MHC-I allele frequencies remained stable, indicating that the observed changes are disease-driven rather than a consequence of neutral drift. Our results show that DFT1 is not only shaping allelic variation within MHC-I loci but is actively reshaping MHC-I gene architecture at the population level. To our knowledge, this constitutes the first empirical demonstration of a naturally occurring disease driving selection against a functional MHC-I locus ("gene death") in a wild vertebrate population, and the first robust genetic evidence, supported by a direct immune phenotype, that Tasmanian devils are co-evolving with a transmissible cancer.

Despite historically low genetic diversity, Tasmanian devils retain sufficient variation for strong selection imposed by DFT1 (Clement et al., 2024; Cunningham et al., 2021; James et al., 2019; Strickland et al., 2024), with eco-evolutionary models predicting long-term host–tumour coexistence rather than extinction (Clement et al., 2024). Previous genome-wide studies have identified signatures of selection following disease emergence (Margres et al., 2018b; Wright et al., 2017), but these have largely been based on genomic or inferential data and have lacked a direct functional link between host genotype and tumour recognition in the wild (Epstein et al., 2016; Margres et al., 2018a). From the tumour perspective, DFT1 has diversified into multiple lineages under strong immune evasion and demographic pressures (Kwon et al., 2020; Stammnitz et al., 2023), with reduced MHC-I expression proposed to arise through pathways such as ERBB3 signalling (Maskell et al., 2025; Schönbichler et al., 2026). Consistent with this, DFT1 cells commonly downregulate surface MHC-I, although expression can be restored under inflammatory conditions such as exposure to interferon-γ (Siddle & Kaufman, 2013). Our findings provide a direct link between these genomic and tumour-intrinsic processes by demonstrating reciprocal evolution along the MHC-I axis: tumours adopt strategies that reduce MHC expression, while hosts evolve MHC-I configurations that increase dissimilarity to the tumour and enhance immune recognition. Together, these results highlight a dynamic coevolutionary interaction in which both host and tumour are actively reshaping MHC architecture under strong contemporary selection.

Our results show that, under extreme and highly specific selective conditions, loss of an entire MHC-I locus can be advantageous, challenging the assumption that greater MHC diversity is always beneficial (Hughes & Nei, 1992; Radwan et al., 2020; Sommer, 2005). In Tasmanian devils, deletion of Saha-UA reduces MHC-I similarity between host and DFT1, increasing the likelihood of allorecognition and anti-tumour immune responses. This differs from the classical interpretation of MHC "death" as a passive consequence of gene duplication, redundancy and relaxed constraint.

Instead, DFT1 appears to be imposing positive selection for a loss-of-function variant that improves immune discrimination of a transmissible cancer.

The evolutionary context is also important. The classical MHC-I genes in devils appear to have arisen through relatively recent duplication events, indicating that this repertoire remains dynamic. Loss of Saha-UA therefore represents not erosion of an ancient, static gene family, but selective pruning of a recently expanded MHC-I repertoire. Together, these findings provide rare empirical evidence that both "birth" and "death" components of MHC evolution can operate over contemporary timescales in response to a single, intense disease pressure. More broadly, they extend the birth-and-death model by showing that gene "death" can be directly favoured by natural selection within populations, rather than inferred only from macroevolutionary comparisons. Similar patterns have been observed in other systems. In deep-sea anglerfishes (Ceratioidei), males attach to females either temporarily or permanently through tissue fusion, creating an extreme challenge to histocompatibility. In species that exhibit permanent attachment, reduced numbers of classical MHC class I genes (*mhc1u*) and expansions of alternative class I lineages (*mhc1z*) have been reported (Swann et al., 2020). These patterns are consistent with reduced histocompatibility barriers facilitating tissue integration, and more broadly suggest that, under certain selective regimes, loss or restructuring of MHC-I loci may be favoured when recognition of non-self is disadvantageous.

Anti–MHC-I antibody responses in Tasmanian devils appear to confer a fitness advantage by extending survival and increasing opportunities for reproduction. In our dataset, six of thirteen devils with anti–MHC-I antibodies and no detectable DFTD were aged four years or older, an uncommon outcome in diseased populations where individuals rarely survive beyond three years (Lazenby et al., 2018), compared to pre-DFTD lifespans of up to seven years (Guiler, 1978). Although immune capacity is known to decline with age (Cheng et al., 2017), the likelihood of repeated exposure to DFT1 increases over time and during mating interactions (Hamede et al., 2013), suggesting that these older, antibody-positive individuals had encountered the tumour multiple times. A similar pattern is seen in a previously reported individual that underwent tumour regression and remained antibody-positive and DFT1-free for at least three years, surviving to six years of age (Pye et al., 2016b). However, antibody responses were not uniformly protective: nearly half of seropositive individuals in our study presented with tumours ranging from early to advanced stages. This variation in outcomes parallels observations in human transplantation biology, where anti-HLA antibodies can mediate rejection, partial control, or chronic pathology depending on their functional properties (Colvin, 2007; Loupy et al., 2013; Stegall et al., 2012). Consistent with this, antibody-mediated responses in devils may not reliably eliminate tumours but could slow tumour growth, thereby extending survival. Even modest increases in survival, permitting an additional breeding season, would generate strong selective pressure on immune phenotypes associated with tumour control, potentially explaining the rapid increase in UA deletion observed over just a few generations. Together, these findings suggest that selection is acting on both genetic variation and functional immune responses, driving contemporary host adaptation to DFT1.

The evolutionary trajectory emerging in Tasmanian devils echoes, on a much shorter timescale, patterns inferred for canine transmissible venereal tumour (CTVT). CTVT is an ancient transmissible

cancer thought to have arisen in populations with low MHC diversity and to have evolved mechanisms that modulate MHC to facilitate transmission (Murgia et al., 2006). Over time, it appears to have reached a relatively stable coexistence with its hosts (Murgia et al., 2006). In contrast, DFTD is evolutionarily recent and occurs in a species with limited MHC-I diversity, resulting in high virulence and strong reciprocal selection on both host and tumour. Our results suggest that early host responses to a transmissible cancer may involve selection for genotypes that reduce similarity to the tumour, including loss of the Saha-UA locus and declines in tumour-matched supertypes. These shifts may represent an initial stage of host adaptation, potentially increasing immune recognition of tumour cells. Whether such changes will ultimately lead to a more stable host–tumour equilibrium, as proposed for CTVT, remains uncertain.

The long-term immunogenetic resilience of Tasmanian devils is likely to depend on retaining sufficient MHC-I diversity to support broader immune function. As a key gene family involved in pathogen recognition, the loss of the Saha-UA gene may enhance resistance to DFT1 but could also have implications for responses to other pathogens. One example of a potential emerging threat is highly pathogenic avian influenza (HPAI) H5N1 2.3.4.4b, which is currently spreading globally and causing significant mortality in birds, poultry, and increasing numbers of mammalian species (Graziosi et al., 2024; Webby & Uyeki, 2024). Transmission has been observed in some systems through contact with infected or dead animals, including in marine mammals. Tasmanian devils, particularly in coastal regions, scavenge a range of species including marine birds (Molloy et al., 2025), and some of these populations (e.g., Stony Head, NNP, wukalina) have a high frequency of the Saha-UA deletion. While there is evidence in other species, such as chickens and pinnipeds, that MHC-I diversity can influence responses to HPAI (Ashley et al., 2026; Hunt et al., 2010), the extent to which these patterns apply to Tasmanian devils remains unclear. Together, these observations suggest that ongoing selection driven by DFT1 may interact with future disease risks in complex ways. Accordingly, conservation strategies may benefit from maintaining immunogenetic variation where possible, for example through managed translocations, while also recognising that alleles associated with DFT1 resistance are likely to be advantageous under current conditions (Fisher et al., 2025; McLennan et al., 2024; Schraven et al., 2025a; Schraven et al., 2025b). Balancing these potentially competing selective pressures will be important for supporting population resilience over time.

In conclusion, this study demonstrates that DFT1 is driving strong, contemporary, and directional evolution of the MHC-I system in Tasmanian devils, including the loss of an entire MHC-I locus. By linking MHC-I genotype to a functional immune phenotype (anti-MHC-I antibody responses) and documenting parallel allele frequency shifts across multiple populations, we provide clear empirical evidence that a naturally occurring disease can drive contemporary MHC gene loss in a vertebrate species. These findings refine our understanding of MHC evolution by showing that, under intense and highly specific selective pressures such as those imposed by a transmissible cancer, contraction of the immune gene repertoire can be adaptive. More broadly, our results highlight that the evolutionary consequences of immune diversity are context dependent. While increased MHC diversity is typically advantageous, transmissible cancers may favour genotypes that reduce host–tumour compatibility. By demonstrating that DFT1 is actively reshaping MHC architecture in the wild, this study provides a foundation for future work linking immune genotype to antibody responses and

fitness outcomes such as survival and reproduction. Understanding how these competing selective pressures interact in natural populations will be increasingly important as disease dynamics shift under global change. Integrating immunogenetics with evolutionary and conservation frameworks will therefore be essential for predicting and managing the long-term resilience of wildlife faced with emerging infectious diseases.

Materials and Methods

Sample collection and non-genetic determinants of an antibody response

Serum samples and ear biopsies were collected from Tasmanian devils during routine health monitoring trips by the Save the Tasmanian Devil Program according to previously described field methods (Lazenby et al., 2018). Samples from the 116 wild devils included in this study were collected between 2015 and 2024 from six sites across Tasmania (Fentonbury, Kempton, Stony Head, wukalina, Granville Harbor and Narawntapu National Park). Individual devils were examined and the sex, weight, head width, reproductive status (females only), tooth eruption and wear, and the presence of DFT1 were recorded. A size-adjusted measure of body weight to head width ratio was used (as a measure of body condition; see Farquharson et al. (2018) for details). Devils were aged using tooth eruption and wear (Jones, 2023). Only devils two years and older were included in this study as DFT1 prevalence is low in younger devils. For DFT1 status, individuals were categorised as 'diseased' when typical tumours were visible and/ or when DFT1 was confirmed by laboratory analysis (e.g. histopathology, fine needle aspirate). All other devils were categorised as 'healthy'. Forty-eight of the 116 devils in this sample set had DFT1. The five non-genetic parameters of location, sex (male = 0, female = 1), body condition, age and DFT1 status (healthy = 0, diseased = 1) were tested for their correlation with the antibody response (Table S1 for metadata). As four of the sites (Buckland, Narawntapu, Stony Head, wukalina) had been genetically managed through supplementation, pedigree reconstruction was used to ensure the individuals in the dataset were not hybrid (see McLennan et al. (2024) for details). Samples were collected under Animal Care and Ethics Committee permits from the University of Sydney (2014/681; 2019/1562; 2022/2243) and the University of Tasmania (A0014976; A0017550; 26159).

Detection of serum anti-DFT1 antibodies

Serum samples were analysed for antibodies against whole DFT1 cells not expressing surface MHC-I, and whole DFT1 cells treated with interferon gamma (IFN-γ) to upregulate surface expression of MHC-I proteins. The method relied on indirect immunofluorescence and flow cytometry and is described in detail in Pye et al. (2016a). In brief, cultured DFT1 cells (cell line C5065) were treated with recombinant devil IFN-γ (5 ng/mL) to induce cell-surface expression of MHC-I, confirmed by flow cytometry with positive staining for the beta 2 microglobulin (B2M) subunit of MHC-I. Serum samples diluted to 1:50 with a flow-cytometry buffer (phosphate-buffered saline with 1% bovine serum albumin and 0.1% sodium azide) were incubated with treated DFT1 cells, and separately with untreated DFT1 cells. After washing, cells were incubated with a monoclonal mouse anti-devil IgG antibody (A4-D1-2). Cells were washed, then incubated with a fluorochrome-labelled goat anti-mouse IgG antibody (Alexa Fluor® 647). After a final wash, cells were resuspended in flow-cytometry buffer containing cell-viability dye (4',6-diamidino-2-phenylindole, dilactate) to allow gating of dead cells, and analysed by flow cytometry (BD Canto II) and FCS Express v7 (DeNovo software).

The median fluorescence intensity ratio (MFIR) was used to classify the antibody responses. The MFIR is defined as the median fluorescence intensity (MFI) of DFT1 cells labelled with immune serum divided by the MFI of DFT1 cells labelled with the negative control serum. The negative control serum samples came from captive devils that had never been exposed to DFT1. This ratio accounts for any background serum IgG present and standardises the responses between individual devils. Antibody responses were classified as positive when the MFIR > 1.5 x MFI of the negative control sample (Pye et al., 2016a). See Fig. 2 for examples of positive and negative antibody responses.

MHC-I typing

DNA was extracted from devil ear biopsies and DFT1 and DFT2 cell lines using the MagAttract HMW DNA kit (Qiagen, Germany). The three functional domains (exons 2, 3 and 4) of the devil MHC-I genes (Saha -*UA*, -*UB*, -*UC*) were amplified following a long-read MHC typing method previously described (Cheng et al., 2022). In brief, the MHC-I genes were amplified using formerly designed forward (/5AmMC6/gcagtcgaacatgtagctgactcaggtcacGTGTCCCCCCCTCCGTCTCAG) and reverse (/5AmMC6/tggatcacttgtgcaagcatcacatcgtagCCTAACTCCCCCTGCTCCTTCTG) primers and the Platinum SuperFi II PCR Master Mix (Invitrogen). Amplicons were indexed using the Barcoded Universal F/R Primers Plate-96v2 (Pacific Biosciences) and the Phusion Hot Start II High Fidelity PCR Master Mix (Thermo Scientific) (see (Cheng et al., 2022) for PCR conditions). Samples were pooled and purified using AMPure PB magnetic beads (Pacific Biosciences), to keep only the target weight molecules. Libraries were prepared using the SMRTbell Express Template Prep Kit 2.0 (Pacific Biosciences) and sequenced on a PacBio Sequel II platform at the Australian Genome Research Facility.

Data processing and MHC genotyping

The raw subread data was processed using the PacBio Secondary Analysis Tools on BioConda (Grüning et al., 2018) (available at https://github.com/PacificBiosciences/pbbioconda), following the methods described in (Cheng et al., 2022). In short, circular consensus sequencing (CCS) reads were generated with --by-strand using ccs v6.4.0 and were filtered to keep reads with a minimum of 5 read passes and read quality ≥ 0.995. Reads were demultiplexed using lima v2.7.1, with concatemer and partial reads removed using isoseq refine v3.8.2. The remaining reads were aligned to the devil MHC-I reference sequence (Saha-UA) using pbalign v0.4.1, with a minimum alignment length of 1300 bp, and mapping quality of 254. As the call rate and accuracy of genotyping has been shown to degrade below 250 reads (Charnaud et al., 2022), individuals with fewer than 250 CCS reads were removed. Alleles were called for each individual using Bellerophon (https://github.com/yuanyuan929/bellerophon) and assigned allele names from a database of known devil MHC-I alleles (Cheng et al., 2022). Alleles were further grouped into known supertypes based on their biochemical properties (see (Cheng et al., 2022)).

A dataset containing genetic variables was generated to test whether an antibody response is influenced by a devil's MHC repertoire. As majority of the MHC variation in devils is driven by CNV, the number of MHC alleles per individual (N_a) was included. As heterozygosity may impact an individual's ability to mount an immune response and is vital to recognising a wide range of

pathogens, we included standardised heterozygosity (H_s) as a genetic variable. This was calculated by dividing the individual observed heterozygosity by the mean observed heterozygosity across all samples, using the 'genhet' package (Coulon, 2010) in R v4.3.1 (R Core Team, 2023). To understand whether a particular gene drives variation in the antibody response, heterozygosity at each gene (coded 1/0 for heterozygote/homozygote), genotypic data (coded as a 0/1 for absence/presence), and supertype data (coded as a 0/1 for absence/presence) were included in the genetic dataset. Only genotypes that were present within at least five individuals were included.

We estimated the overall genetic similarity (D_{AB}) between self and non-self at the allele and supertype level. All individuals included in this study were captured at sites where only DFT1 is currently present. We therefore calculated genetic similarity between the host and DFT1 only, as per (Brandies et al., 2018). The overall D_{AB} (similarity at the three MHC genes) between an individual and DFT1 was calculated using Wetton's formula: $D_{AB} = 2F_{AB}/(F_A + F_B)$ (Wetton et al., 1987). Here, F_{AB} is the total number of shared alleles or supertypes between DFT1 and an individual, and F_A and F_B are the total number of alleles or supertypes of DFT1 (A) and an individual (B). We also tested whether the D_{AB} at each gene had a greater influence on the antibody response than the overall MHC similarity.

Modelling the effects of the MHC-I repertoire on antibody responses

Generalised Linear Models (GLM) were generated using the 'glm' function in R to predict which variable had the strongest effect on the logistic response variable (antibody response). We ran multiple models to understand whether 1) non-genetic variables influenced the antibody response (antibody response ~ age + sex + body condition + disease status + site), 2) MHC-I influenced the antibody response and 3) a particular genotype influenced the antibody response (Supp for all models). We used an information theoretic approach to model selection using AICc (corrected Akaike information criterion) and averaging of the top models following (Grueber et al., 2011). Models were ranked based on their AICc values, with models <2 AICc from the top model considered to influence the antibody response. Where multiple models best described the data (non-genetic variables), only the top models (Δ AICc < 2) were selected, and the relative importance (RI) of predictors was calculated using the 'MuMIn 1.47.5' R package (Bartoń, 2023). Only predictors with a RI = 1 (equivalent to the predictor appearing in all top models) were considered well supported. For all genetic variables, only one top model best described the data. Therefore, the model effect sizes, their standard errors and P-values (α=0.05), were used to infer the importance of predictors. Model predictors were standardised by subtracting the mean and diving by one standard deviation. The relationship between -UA genotypes and antibody responses were visualised by clustering devils and DFT1 (based on their -UA genotype) using the 'Factoextra' R package (Kassambara & Mundt, 2020).

Transplant score model

Antibody response was analysed against UA/UB/UC supertype allele score using logistic regression. The allele score was derived by summing presence of allele scores over UA, UB and UC, whereby a complete allele match with DFT1 was scored 0, and a complete mismatch was scored 6. Probabilities of antibody response for high and low allele score were obtained from generalized linear models (glm) using a binomial error distribution and link function in R v4.4.0. (R Core Team,

2023). The ggplot2 was package was used to make transplant score plots showing the shaded 95% confidence intervals around the regression trend lines (Wickham, 2011).

Temporal analysis

Changes in supertype frequencies at disease and disease-free sites over time were visualised using R v4.1.1. (R Core Team, 2023). The 592 samples were collected between 2012 and 2021. All individuals included in the temporal analysis were non-translocated devils and non-hybrids. To estimate the overall temporal pattern across locations of deletion UA allele or presence of super-type 2 and super-type 7, we used logistic regression of these variables against years since DFTD introduction, accounting for non-independence within locations by using clustering-robust standard errors. A non-linear effect for years since DFTD introduction (first time devil appeared in the data) was included using natural cubic spline with three degrees of freedom. Additionally, location-specific temporal trends were estimated using a separate logistic regression model that included an interaction between years since DFTD introduction and location. In both modelling approaches, probabilities of presence or deletion for each year since DFTD introduction were obtained from model-based expected values.

Evidence of MHC birth in devils

In order to identify evidence of devil specific MHC class I duplication(birth) we first used biser (Išerić et al., 2022) to locate segmental duplications within the Tasmanian devil reference genome (GCF_902635505.1). We then filtered down the results to identify duplications involving the classical class I genes on scaffold NC_045429.1.

Secondly, given the high sequence similarity between the three classical genes (UA, UB and UC) we aimed to estimate the potential duplication dates of these three genes. Using the formula $d=2\mu t$ (where d is sequence divergence, μ is mutation rate and t is time), along with the devil specific yearly mutation rate of 1.98×10^{-9} mutations/bp/year (1.92×10^{-9}-3.98×10^{-9}). We used PAML v4.10.9 to calculate the dS ratio between all devil MHC genes (UA, UB, UC, UD, UK and UM) and then used this value for sequence divergence and rearranged the above formula to $t= d/2\mu$. We estimated divergence times between the three genes using the average as well as the upper and lower 95% CI for the mutation rate. We used dS for divergence time as an assumption of the divergence formula is that sites are evolving neutrally, as MHC genes evolve under high selective pressures including sites with non-synonymous mutations would violate this principle whereas sites with synonymous mutations can be assumed to be evolving neutrally.

Acknowledgements

We acknowledge the traditional custodians of the land on which these devil (purinina) populations live and pay respects to their elders past and present. We thank the various current and past staff of the Save the Tasmanian Devil Program who have undertaken extensive monitoring of devil sites and participated sample collection, in particular Samantha Fox, Drew Lee, Billie Lazenby, Jodie Elmer, David Schaap, Bill Brown, Stewart Huxtable, Clare Lawrence, and Phil Wise. We also thank Petr Otahal with assistance with some of the modelling analysis and Chrissie Ong, Jocelyn Darby, and Alexandra Sharland for guidance on MHC immunology and laboratory assays, and Andrea Schraven for the neutral diversity data. This work was supported by the Australian Research Council [LP180100244, LE240100080], the University of Sydney, the Save the Tasmanian Devil Program and San Diego Zoo Wildlife Alliance. KF and LS are supported by funding from the ARC Centre of Excellence for Innovations in Peptide and Protein Science (CE200100012). AF was supported by the Select Foundation and ARC FT240100092.

Data availability

All raw sequence data have been deposited onto Dryad and will be made public following acceptance of this manuscript.

Benefit-Sharing Statement

A research collaboration exists between academics and the Department of Natural Resources and Environment Tasmania (NRE Tas), who provided operational and logistical support, including access to information and genetic samples to undertake this study. The results of the research have been shared with the NRE Tas in real-time to inform their management actions for the conservation of the Tasmanian devil. NRE Tas engage with local Indigenous communities and other local communities in relation to management of the species.

Conflict of interest

The authors declare no conflicting interests.

Author contributions

Conceptualisation, C.J.H, K.B., A.S.F., R.J.P.; Fieldwork, R.J.P., K.C.B., C.J.H.; Lab work, K.C.B., R.J.P., Y.C., Data analysis, K.C.B., R.J.P., L.S., K.A.F., Y.C., A.S.F.; Writing – Original Draft, K.C.B., R.J.P., C.J.H.; Writing – Review and Editing, all authors; Visualisation, K.C.B., R.J.P., L.S., C.J.H.; Supervision, C.J.H., K.B., A.S.F.; Resources, C.J.H., K.B., A.S.F; Funding acquisition, C.J.H., K.B., A.S.F.

References

Barker, D. J., Maccari, G., Georgiou, X., Cooper, M. A., Flicek, P., Robinson, J., & Marsh, S. G. (2023). The IPD-IMGT/HLA database. *NUCLEIC ACIDS RESEARCH*, *51*(D1), D1053-D1060.

Bartoń, K. (2023). MuMIn: Multi-Model Inference_. R package version 1.47.5. https://CRAN.R-project.org/package=MuMIn.

Belov, K. (2011). The role of the Major Histocompatibility Complex in the spread of contagious cancers. *MAMMALIAN GENOME*, *22*(1-2), 83-90. https://doi.org/10.1007/s00335-010-9294-2

Belov, K. (2012). Contagious cancer: Lessons from the devil and the dog. *BIOESSAYS*, *34*(4), 285-292. https://doi.org/10.1002/bies.201100161

Bjorkman, P. J., & Parham, P. (1990). Structure, function, and diversity of class I major histocompatibility complex molecules. *Annual review of biochemistry*, *59*, 253-288.

Brandies, P. A., Grueber, C. E., Ivy, J. A., Hogg, C. J., & Belov, K. (2018). Disentangling the mechanisms of mate choice in a captive koala population. *PEERJ*, *6*, e5438. https://doi.org/10.7717/peerj.5438

Charnaud, S., Munro, J. E., Semenec, L., Mazhari, R., Brewster, J., Bourke, C., Ruybal-Pesántez, S., James, R., Lautu-Gumal, D., Karunajeewa, H., Mueller, I., & Bahlo, M. (2022). PacBio long-read amplicon sequencing enables scalable high-resolution population allele typing of the complex CYP2D6 locus. *COMMUNICATIONS BIOLOGY*, *5*(1), 168. https://doi.org/10.1038/s42003-022-03102-8

Cheng, Y., Grueber, C., Hogg, C. J., & Belov, K. (2022). Improved high-throughput MHC typing for non-model species using long-read sequencing. *MOLECULAR ECOLOGY RESOURCES*, *22*(3), 862-876. https://doi.org/https://doi.org/10.1111/1755-0998.13511

Cheng, Y., Stuart, A., Morris, K., Taylor, R., Siddle, H., Deakin, J., Jones, M., Amemiya, C. T., & Belov, K. (2012a). Antigen-presenting genes and genomic copy number variations in the Tasmanian devil MHC. *BMC GENOMICS*, *13*, Article 87. https://doi.org/10.1186/1471-2164-13-87

Cheng, Y. Y., & Belov, K. (2014). Characterisation of non-classical MHC class I genes in the Tasmanian devil (*Sarcophilus harrisii*). *Immunogenetics* *66*(12), 727-735. https://doi.org/10.1007/s00251-014-0804-3

Cheng, Y. Y., Sanderson, C., Jones, M., & Belov, K. (2012b). Low MHC class II diversity in the Tasmanian devil (*Sarcophilus harrisii*). *IMMUNOGENETICS*, *64*(7), 525-533. https://doi.org/10.1007/s00251-012-0614-4

Coulon, A. (2010). GENHET: an easy-to-use R function to estimate individual heterozygosity. *MOLECULAR ECOLOGY RESOURCES*, *10*(1), 167-169. https://doi.org/10.1111/j.1755-0998.2009.02731.x

Cresswell, P., Ackerman, A. L., Giodini, A., Peaper, D. R., & Wearsch, P. A. (2005). Mechanisms of MHC class I-restricted antigen processing and cross-presentation. *Immunological reviews*, *207*(1), 145-157.

Cunningham, C. X., Comte, S., McCallum, H., Hamilton, D. G., Hamede, R., Storfer, A., Hollings, T., Ruiz-Aravena, M., Kerlin, D. H., Brook, B. W., Hocking, G., & Jones, M. E. (2021). Quantifying 25 years of disease-caused declines in Tasmanian devil populations: host density drives spatial pathogen spread. *ECOLOGY LETTERS*, *24*(5), 958-969. https://doi.org/10.1111/ele.13703

Duchêne, D. A., Bragg, J. G., Duchêne, S., Neaves, L. E., Potter, S., Moritz, C., Johnson, R. N., Ho, S. Y. W., & Eldridge, M. D. B. (2018). Analysis of Phylogenomic Tree Space Resolves Relationships Among Marsupial Families. *Systematic Biology*, *67*(3), 400-412. https://doi.org/10.1093/sysbio/syx076

Farquharson, K. A., Gooley, R. M., Fox, S., Huxtable, S. J., Belov, K., Pemberton, D., Hogg, C. J., & Grueber, C. E. (2018). Are any populations 'safe'? Unexpected reproductive decline in a population of Tasmanian devils free of devil facial tumour disease. *WILDLIFE RESEARCH*, *45*(1), 31-37. https://doi.org/10.1071/WR16234

Fox, S., & Seddon, P. J. (2019). Wild devil recovery: managing devils in the presence of disease. In: . In C. J. Hogg, S. Fox, D. Pemberton, & K. Belov (Eds.), *Saving the Tasmanian devil: Recovery through science-based management* (pp. 157-163). CSIRO Publishing. https://doi.org/10.1111/avj.12914

Grueber, C. E., Nakagawa, S., Laws, R. J., & Jamieson, I. G. (2011). Multimodel inference in ecology and evolution: challenges and solutions (vol 24, pg 699, 2011). *Journal of Evolutionary Biology*, *24*(7), 1627-1627. https://doi.org/10.1111/j.1420-9101.2011.02328.x

Grüning, B., Dale, R., Sjödin, A., Chapman, B. A., Rowe, J., Tomkins-Tinch, C. H., Valieris, R., Köster, J., & Team, B. (2018). Bioconda: sustainable and comprehensive software distribution for the life sciences. *Nature Methods*, *15*(7), 475-476. https://doi.org/10.1038/s41592-018-0046-7

Hamede, R. K., McCallum, H., & Jones, M. (2013). Biting injuries and transmission of Tasmanian devil facial tumour disease. *JOURNAL OF ANIMAL ECOLOGY*, *82*(1), 182-190. https://doi.org/10.1111/j.1365-2656.2012.02025.x

Hughes, A. L., & Nei, M. (1992). Maintenance of MHC polymorphism. *NATURE*, *355*(6359), 402-403. https://doi.org/10.1038/355402b0

Hussey, K., Caldwell, A., Kreiss, A., Skjodt, K., Gastaldello, A., Pye, R., Hamede, R., Woods, G. M., & Siddle, H. V. (2022). Expression of the Nonclassical MHC Class I, Saha-UD in the Transmissible Cancer Devil Facial Tumour Disease (DFTD). *PATHOGENS*, *11*(3), Article 351. https://doi.org/10.3390/pathogens11030351

Išerić, H., Alkan, C., Hach, F., & Numanagić, I. (2022). Fast characterization of segmental duplication structure in multiple genome assemblies. *Algorithms for Molecular Biology*, *17*(1), 4. https://doi.org/10.1186/s13015-022-00210-2

Jones, M. E. (2023). Over-eruption in marsupial carnivore teeth: compensation for a constraint. *Proceedings. Biological Sciences / The Royal Society*, *290*(2013), 20230644. https://doi.org/10.1098/rspb.2023.0644

Kassambara, A., & Mundt, F. (2020). Factoextra: Extract and Visualize the Results of Multivariate Data Analyses. R Package Version 1.0.7. https://CRAN.R-project.org/package=factoextra.

Kok, G., Ilcken, E. F., Houwen, R. H., Lindemans, C. A., Nieuwenhuis, E. E., Spierings, E., & Fuchs, S. A. (2023). The effect of genetic HLA matching on liver transplantation outcome: a systematic review and meta-analysis. *Annals of Surgery Open*, *4*(3), e334.

Kreiss, A., Cheng, Y. Y., Kimble, F., Wells, B., Donovan, S., Belov, K., & Woods, G. M. (2011). Allorecognition in the Tasmanian Devil (Sarcophilus harrisii), an Endangered Marsupial Species with Limited Genetic Diversity. *PLOS ONE*, *6*(7), Article e22402. https://doi.org/10.1371/journal.pone.0022402

Kwon, Y. M., Gori, K., Park, N., Potts, N., Swift, K., Wang, J. H., Stammnitz, M. R., Cannell, N., Baez-Ortega, A., Comte, S., Fox, S., Harmsen, C., Huxtable, S., Jones, M., Kreiss, A., Lawrence, C., Lazenby, B., Peck, S., Pye, R.,...Murchison, E. P. (2020). Evolution and lineage dynamics of a transmissible cancer in Tasmanian devils. *PLOS BIOLOGY*, *18*(11), Article e3000926. https://doi.org/10.1371/journal.pbio.3000926

Lachish, S., Jones, M., & McCallum, H. (2007). The impact of disease on the survival and population growth rate of the Tasmanian devil. *JOURNAL OF ANIMAL ECOLOGY*, *76*(5), 926-936. https://doi.org/10.1111/j.1365-2656.2007.01272.x

Laging, M., Kal-van Gestel, J. A., Haasnoot, G. W., Claas, F. H., van de Wetering, J., IJzermans, J. N., Weimar, W., & Roodnat, J. I. (2014). Transplantation results of completely HLA-mismatched living and completely HLA-matched deceased-donor kidneys are comparable. *Transplantation*, *97*(3), 330-336.

Lau, Q., Igawa, T., Kosch, T. A., Dharmayanthi, A. B., Berger, L., Skerratt, L. F., & Satta, Y. (2023). Conserved evolution of MHC supertypes among Japanese frogs suggests selection for Bd resistance. *ANIMALS*, *13*(13), 2121.

Lazenby, B. T., Tobler, M. W., Brown, W. E., Hawkins, C. E., Hocking, G. J., Hume, F., Huxtable, S., Iles, P., Jones, M. E., Lawrence, C., Thalmann, S., Wise, P., Williams, H., Fox, S., & Pemberton, D. (2018). Density trends and demographic signals uncover the long-term impact of transmissible cancer in Tasmanian devils. *JOURNAL OF APPLIED ECOLOGY*, *55*(3), 1368-1379. https://doi.org/10.1111/1365-2664.13088

Loh, R., Bergfeld, J., Hayes, D., O'Hara, A., Pyecroft, S., Raidal, S., & Sharpe, R. (2006a). The pathology of devil facial tumor disease (DFTD) in Tasmanian devils (*Sarcophilus harrisii*). *VETERINARY PATHOLOGY*, *43*(6), 890-895. https://doi.org/10.1354/vp.43-6-890

Loh, R., Hayes, D., Mahjoor, A., O'Hara, A., Pyecroft, S., & Raidal, S. (2006b). The immunohistochemical characterization of devil facial tumor disease (DFTD) in the Tasmanian Devil (*Sarcophilus harrisii*). *VETERINARY PATHOLOGY*, *43*(6), 896-903. https://doi.org/10.1354/vp.43-6-896

Maccari, G., Robinson, J., Barker, D. J., Yates, A. D., Hammond, J. A., & Marsh, S. G. (2025). The 2024 IPD-MHC database update: a comprehensive resource for major histocompatibility complex studies. *NUCLEIC ACIDS RESEARCH*, *53*(D1), D457-D461.

McLennan, E. A., Cheng, Y., Farquharson, K. A., Grueber, C. E., Elmer, J., Alexander, L., Fox, S., Belov, K., & Hogg, C. J. (2024). Reinforcements in the face of ongoing threats: a case study from a critically small carnivore population. *ANIMAL CONSERVATION*. https://doi.org/10.1111/acv.12945

Minias, P., Pikus, E., Whittingham, L. A., & Dunn, P. O. (2019). Evolution of copy number at the MHC varies across the avian tree of life. *GENOME BIOLOGY AND EVOLUTION*, *11*(1), 17-28.

Morris, K., Austin, J. J., & Belov, K. (2013). Low major histocompatibility complex diversity in the Tasmanian devil predates European settlement and may explain susceptibility to disease epidemics. *BIOLOGY LETTERS*, *9*(1), Article 20120900. https://doi.org/10.1098/rsbl.2012.0900

Müller-Klein, N., Risely, A., Wilhelm, K., Riegel, V., Manser, M., Clutton-Brock, T., Silver, L., Santos, P. S. C., Melville, D. W., & Sommer, S. (2025). Twenty years of tuberculosis-driven selection shaped the evolution of the

meerkat major histocompatibility complex. *NATURE ECOLOGY & EVOLUTION*, *9*(11), 2161-2172. https://doi.org/10.1038/s41559-025-02837-x

Murchison, E. P., Wedge, D. C., Alexandrov, L. B., Fu, B., Martincorena, I., Ning, Z., Tubio, J. M., Werner, E. I., Allen, J., & De Nardi, A. B. (2014). Transmissible dog cancer genome reveals the origin and history of an ancient cell lineage. *SCIENCE*, *343*(6169), 437-440.

Murgia, C., Pritchard, J. K., Kim, S. Y., Fassati, A., & Weiss, R. A. (2006). Clonal origin and evolution of a transmissible cancer. *CELL*, *126*(3), 477-487.

Nei, M., Gu, X., & Sitnikova, T. (1997). Evolution by the birth-and-death process in multigene families of the vertebrate immune system. *Proceedings of the National Academy of Sciences*, *94*(15), 7799-7806.

Ong, C. E. B., Patchett, A. L., Darby, J. M., Chen, J. Y., Liu, G. S., Lyons, A. B., Woods, G. M., & Flies, A. S. (2021). NLRC5 regulates expression of MHC-I and provides a target for anti-tumor immunity in transmissible cancers. *JOURNAL OF CANCER RESEARCH AND CLINICAL ONCOLOGY*, *147*(7), 1973-1991. https://doi.org/10.1007/s00432-021-03601-x

Pearse, A. M., & Swift, K. (2006). Transmission of devil facial-tumour disease - An uncanny similarity in the karyotype of these malignant tumours means that they could be infective. *NATURE*, *439*(7076), 549-549. https://doi.org/10.1038/439549a

Pye, R., Hamede, R., Siddle, H. V., Caldwell, A., Knowles, G. W., Swift, K., Kreiss, A., Jones, M. E., Lyons, A. B., & Woods, G. M. (2016a). Demonstration of immune responses against devil facial tumour disease in wild Tasmanian devils. *BIOLOGY LETTERS*, *12*(10), Article 20160553. https://doi.org/10.1098/rsbl.2016.0553

Pye, R. J., Pemberton, D., Tovar, C., Tubio, J. M. C., Dun, K. A., Fox, S., Darby, J., Hayes, D., Knowles, G. W., Kreiss, A., Siddle, H. V. T., Swift, K., Lyons, A. B., Murchison, E. P., & Woods, G. M. (2016b). A second transmissible cancer in Tasmanian devils. *PROCEEDINGS OF THE NATIONAL ACADEMY OF SCIENCES OF THE UNITED STATES OF AMERICA*, *113*(2), 374-379. https://doi.org/10.1073/pnas.1519691113

R Core Team. (2023). R: A Language and Environment for Statistical Computing, https://www.R-project.org/.

Radwan, J., Babik, W., Kaufman, J., Lenz, T. L., & Winternitz, J. (2020). Advances in the evolutionary understanding of MHC polymorphism. *TRENDS IN GENETICS*, *36*(4), 298-311.

Siddle, H. V., & Kaufman, J. (2013). How the devil facial tumor disease escapes host immune responses. *ONCOIMMUNOLOGY*, *2*(8), Article e25235. https://doi.org/10.4161/onci.25235

Siddle, H. V., & Kaufman, J. (2015). Immunology of naturally transmissible tumours. *IMMUNOLOGY*, *144*(1), 11-20. https://doi.org/10.1111/imm.12377

Siddle, H. V., Kreiss, A., Eldridge, M. D. B., Noonan, E., Clarke, C. J., Pyecroft, S., Woods, G. M., & Belov, K. (2007). Transmission of a fatal clonal tumor by biting occurs due to depleted MHC diversity in a threatened carnivorous marsupial. *PROCEEDINGS OF THE NATIONAL ACADEMY OF SCIENCES OF THE UNITED STATES OF AMERICA*, *104*(41), 16221-16226. https://doi.org/10.1073/pnas.0704580104

Siddle, H. V., Kreiss, A., Tovar, C., Yuen, C. K., Cheng, Y. Y., Belov, K., Swift, K., Pearse, A. M., Hamede, R., Jones, M. E., Skjodt, K., Woods, G. M., & Kaufman, J. (2013). Reversible epigenetic down-regulation of MHC molecules by devil facial tumour disease illustrates immune escape by a contagious cancer. *PROCEEDINGS OF THE NATIONAL ACADEMY OF SCIENCES OF THE UNITED STATES OF AMERICA*, *110*(13), 5103-5108. https://doi.org/10.1073/pnas.1219920110

Silver, L. W., Hogg, C. J., & Belov, K. (2024). Plethora of new marsupial genomes informs our knowledge of marsupial MHC class II. *GENOME BIOLOGY AND EVOLUTION*, *16*(8), evae156.

Sommer, S. (2005). The importance of immune gene variability (MHC) in evolutionary ecology and conservation. *Frontiers in zoology*, *2*(1), 16.

Stammnitz, M. R., Gori, K., Kwon, Y. M., Harry, E., Martin, F. J., Billis, K., Cheng, Y. Y., Baez-Ortega, A., Chow, W., Comte, S., Eggertsson, H., Fox, S., Hamede, R., Jones, M., Lazenby, B., Peck, S., Pye, R., Quail, M. A., Swift, K.,...Murchison, E. P. (2023). The evolution of two transmissible cancers in Tasmanian devils. *SCIENCE*, *380*(6642), 283-293. https://doi.org/10.1126/science.abq6453

Tovar, C., Pye, R. J., Kreiss, A., Cheng, Y. Y., Brown, G. K., Darby, J., Malley, R. C., Siddle, H. V. T., Skjodt, K., Kaufman, J., Silva, A., Morelli, A. B., Papenfuss, A. T., Corcoran, L. M., Murphy, J. M., Pearse, M. J., Belov, K., Lyons, A. B., & Woods, G. M. (2017). Regression of devil facial tumour disease following immunotherapy in immunised Tasmanian devils. *SCIENTIFIC REPORTS*, *7*, Article 43827. https://doi.org/10.1038/srep43827

Tran, T. H., Döhler, B., Heinold, A., Scherer, S., Ruhenstroth, A., & Opelz, G. (2011). Deleterious impact of mismatching for human leukocyte antigen-C in presensitized recipients of kidney transplants. *Transplantation*, *92*(4), 419-425.

Trowsdale, J., & Parham, P. (2004). Mini-review: Defense strategies and immunity-related genes. *EUROPEAN JOURNAL OF IMMUNOLOGY*, *34*(1), 7-17.

Wetton, J. H., Carter, R. E., Parkin, D. T., & Walters, D. (1987). Demographic study of a wild house sparrow population by DNA fingerprinting. *NATURE*, *327*(6118), 147-149. https://doi.org/10.1038/327147a0

Wickham, H. (2011). ggplot2. *Wiley interdisciplinary reviews: computational statistics*, *3*(2), 180-185.

Table 1. Age-structured shifts in MHC-I composition reveal selection against tumour-matching genotypes in wild Tasmanian devils.
(A) Frequency of the non-functional *Saha-UA* allele (UA deletion),
(B) frequency of supertype 2 (ST2; shared with DFT1), and
(C) frequency of common UA supertypes not shared with DFT1 (including supertypes 1 and 7 and the UA deletion), across age classes and sampling sites.

Across DFT1-affected populations, older devils are increasingly enriched for the non-functional UA allele and supertypes not shared with the tumour, while the frequency of tumour-matching supertype 2 declines with age. This pattern is consistent with directional selection favouring host–tumour MHC-I dissimilarity, with individuals carrying mismatched genotypes more likely to survive to older age classes. In contrast, frequencies remain relatively stable across age classes at the DFT1-free site (Woolnorth), supporting a disease-driven rather than neutral process.

Shaded boxes indicate missing data; numbers in parentheses indicate sample sizes for each age class.

Sampling site	1 yr old	2 yr old	3 yr old	4 yr old	5 yr old	6 yr old	7 yr old
A) Non-functional UA allele							
Bronte	0.47 (29)	0.43 (14)	0.63 (4)	0.00 (1)			
Buckland	0.18 (30)	0.20 (15)	0.50 (4)				
Fentonbury	0.6 (20)	0.48 (33)	0.34 (16)	0.75 (2)		0.50 (1)	
Granville	0.27 (26)	0.46 (12)	0.50 (6)	0.50 (1)			
Kempton	0.67 (12)	0.27 (15)	0.50 (10)	0.70 (5)	1.00 (2)		
NNP	0.40 (29)	0.71 (17)	0.67 (6)		0.50 (1)		1.00 (1)
SH	0.35 (128)	0.34 (35)	0.53 (18)	0.50 (2)		1.00 (1)	
Woolnorth	0.35 (17)	0.18 (11)	0.29 (7)	0.19 (8)	0.19 (13)	0.00 (2)	
wukalina	0.68 (22)	0.59 (11)	0.70 (5)				
B) Supertype 2 (shared with DFT1)							
Bronte	0.26	0.36	0.25	0.00			
Buckland	0.57	0.60	0.38				
Fentonbury	0.20	0.32	0.47	0.25		0.00	
Granville	0.56	0.50	0.25	0.00			
Kempton	0.17	0.3	0.15	0.00	0.00		
NNP	0.31	0.21	0.17		0.00		0.00
SH	0.64	0.64	0.47	0.50		0.00	
Woolnorth	0.62	0.82	0.50	0.81	0.77	0.75	
wukalina	0.27	0.36	0.20				
C) Common UA supertypes (excluding ST2)							
Bronte	0.72	0.64	0.75	1.00			
Buckland	0.37	0.30	0.50				
Fentonbury	0.80	0.68	0.53	0.75		1.00	
Granville	0.42	0.5	0.75	1.00			
Kempton	0.83	0.63	0.8	1.00	1.00		
NNP	0.53	0.74	0.83		1.00		1.00
SH	0.36	0.36	0.53	0.50		1.00	
Woolnorth	0.38	0.18	0.36	0.19	0.23	0.25	
wukalina	0.70	0.59	0.80				

725

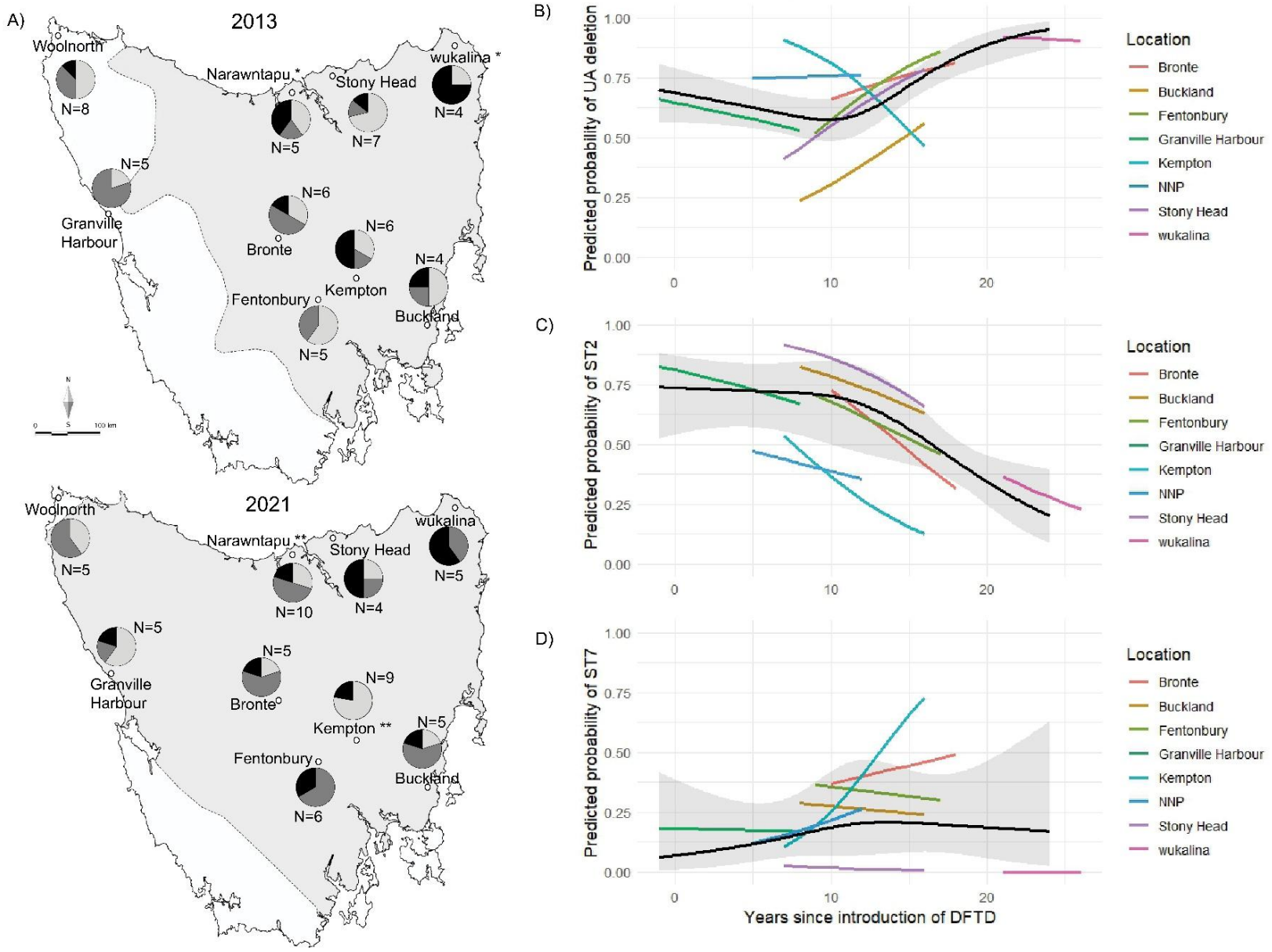

A)
2013
Woolnorth
N=8
Narawntapu *
N=5
Stony Head
N=7
wukalina *
N=4
N=5
Granville Harbour
N=6
Bronte
N=6
Kempton
N=4
Buckland
Fentonbury
N=5
2021
Woolnorth
N=5
Narawntapu **
N=10
Stony Head
N=4
wukalina
N=5
N=5
Granville Harbour
N=5
Bronte
N=9
Kempton **
N=5
Buckland
Fentonbury
N=6
B)
Predicted probability of UA deletion
C)
Predicted probability of ST2
D)
Predicted probability of ST7
0.00
0.25
0.50
0.75
1.00
0
10
20
Years since introduction of DFTD
Location
Bronte
Buckland
Fentonbury
Granville Harbour
Kempton
NNP
Stony Head
wukalina

Fig. 1. Disease-driven shifts in MHC-I composition across Tasmanian devil populations following the spread of DFT1.

(A) Spatial distribution of the non-functional Saha-UA allele (UA deletion) across Tasmania in 2013 and 2021. Pie charts show genotype frequencies (light grey = two functional UA alleles, dark grey = one deletion, black = homozygous deletion), with shading indicating the position of the disease front at each time point.

(B–D) Temporal trajectories of key MHC-I variants plotted as predicted probabilities from model-based expected values against years since DFT1 arrival at each site (coloured lines), with overall trends across sites shown in black (± SE, grey shading).

(B) Probability of the UA deletion increases over time following disease arrival, indicating selection for loss of the Saha-UA locus.
(C) Probability of supertype 2 (ST2; shared with DFT1) declines across sites, consistent with selection against tumour-matching genotypes.
(D) Probability of supertype 7 (ST7; not shared with DFT1) shows a modest increase, reflecting enrichment of tumour-mismatched genotypes.

Across multiple independently affected populations, these parallel trends demonstrate directional selection favouring host–tumour MHC-I dissimilarity, with loss of Saha-UA and decline of tumour-matching supertypes occurring over just a few generations.

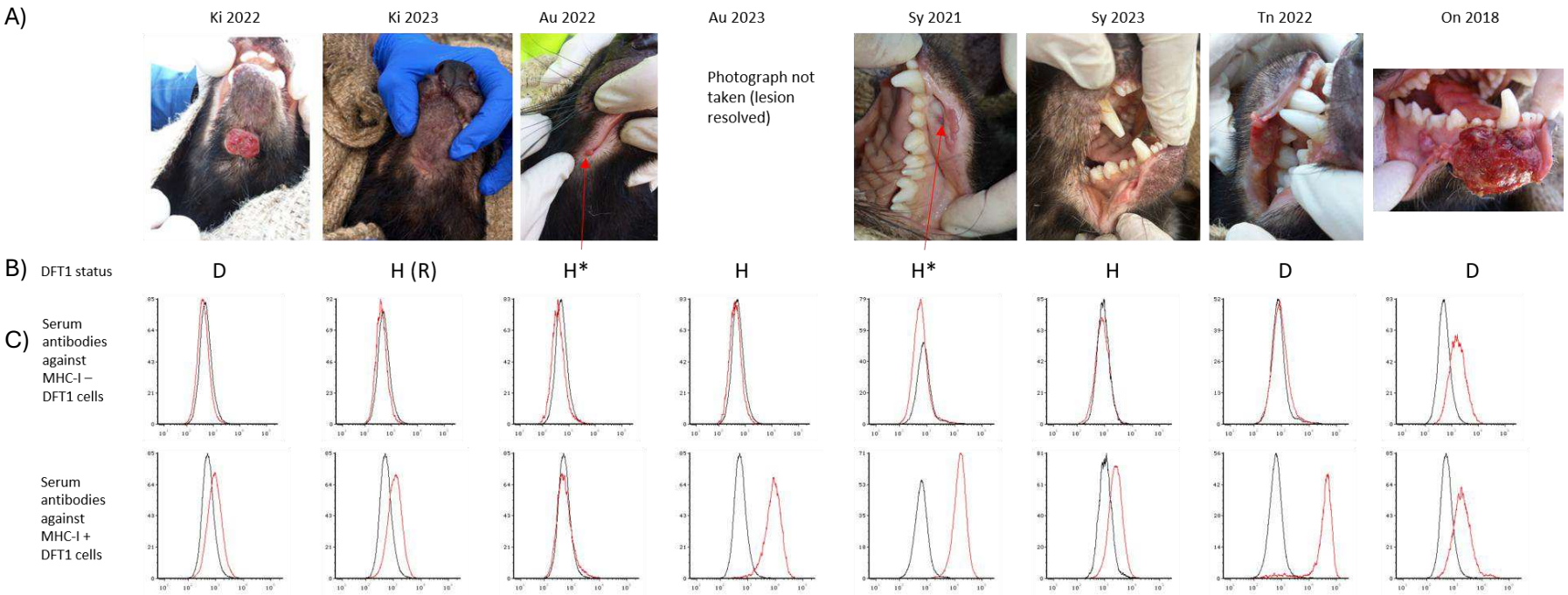


Fig. 2. Anti–MHC-I antibody responses in wild Tasmanian devils with and without DFT1.
Representative examples of five individual devils illustrating variation in clinical status and antibody responses to DFT1 cells. For each individual, A) shows the animal and any visible tumour or lesion, followed by B) clinical status (D = DFT1 present; H = healthy; H(R) = healthy following tumour regression; H* = suspected but unconfirmed lesion). C) Flow cytometry histograms show serum antibody binding to DFT1 cells lacking surface MHC-I (MHC-I–; fourth row) and to DFT1 cells induced to express MHC-I (MHC-I+; bottom row). Antibody binding from each devil (red) is compared to a naïve control (black); a rightward shift indicates a positive response.

Across individuals, antibody responses are typically detected against MHC-I+ but not MHC-I– tumour cells, demonstrating that anti-tumour immunity is primarily directed against MHC-I. Notably, antibody-positive individuals include devils that have remained disease-free following exposure or undergone tumour regression, consistent with a functional immune response associated with improved outcomes.

Sex, age, and sampling location for each individual are provided in Table S1.

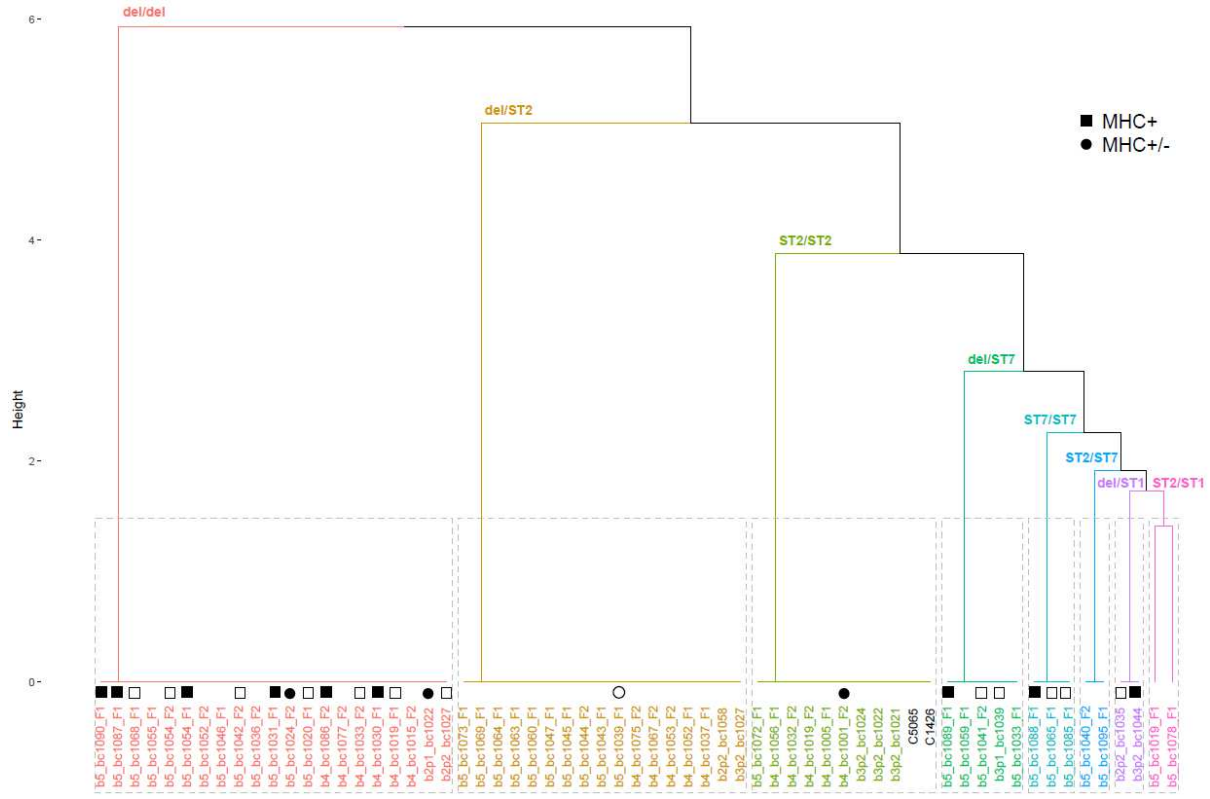


Fig. 3. MHC-I genotype determines immune recognition of transmissible tumour cells in wild Tasmanian devils.

Hierarchical clustering of Tasmanian devils and DFT1 cell lines based on UA genotype. Labels above branches denote UA genotype classes (del = deletion; ST = supertype), and labels below identify individual devils; black labels (C5065 and C1426) represent DFT1 cell lines.

Symbols indicate antibody responses: squares represent individuals with antibodies against MHC-I+ DFT1 cells only, circles represent individuals with antibodies against both MHC-I+ and MHC-I– cells. Filled symbols denote devils with clinical DFT1; unfilled symbols denote animals with no clinical disease.

Most devils with anti-DFT1 antibody responses cluster separately from the tumour and lack UA genotypes shared with DFT1, demonstrating that MHC-I genotype mismatch between host and tumour is strongly associated with immune recognition. In contrast, devils sharing tumour-associated genotypes (e.g. supertype 2) show reduced or altered antibody responses, consistent with decreased immunogenicity of matched tumours.

A small number of ST2 individuals exhibit antibody binding to MHC-I– cells, suggesting the presence of non–MHC-I tumour antigens in these cases.

Supplementary Files

This is a list of supplementary files associated with this preprint. Click to download.

- TableS1final.xlsx
- DevilMHCsupplementary.docx